ChemComm

Chemical Communications

www.rsc.org/chemcomm

Volume 46 | Number 10 | 14 March 2010 | Pages 1565–1776

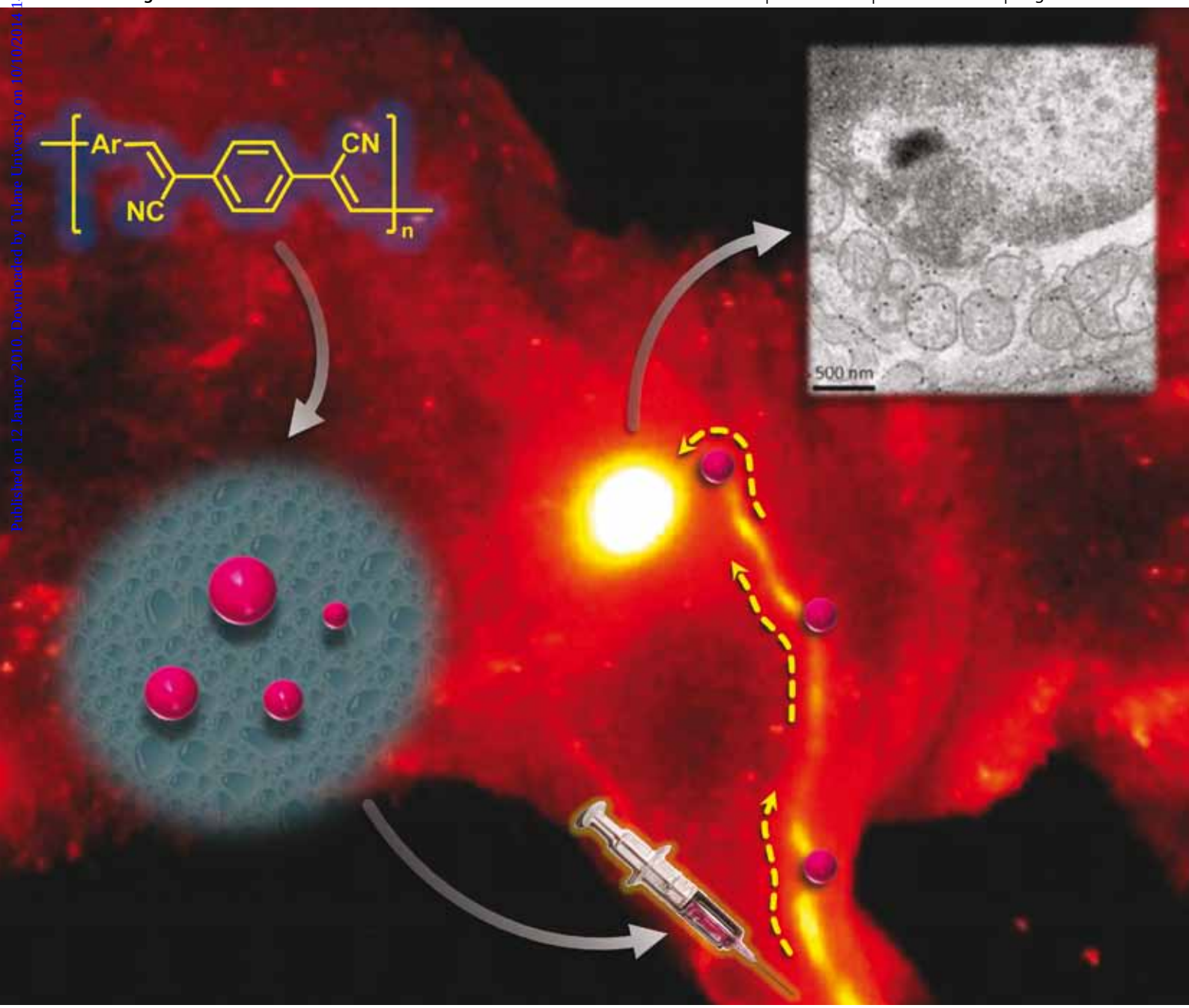

ISSN 1359-7345

RSC Publishing

1359-7345(2010)46:10;1-P

Conjugated polymer nanoparticles for biomedical *in vivo* imaging†

Sehoon Kim,*[a] Chang-Keun Lim,[a] Jinhee Na,[a] Yong-Deok Lee,[a] Kwangmeyung Kim,[a] Kuiwon Choi,[a] James F. Leary[b] and Ick Chan Kwon[a]

Received (in Cambridge, UK) 6th November 2009, Accepted 11th December 2009
First published as an Advance Article on the web 12th January 2010
DOI: 10.1039/b923309a

Conjugated polymer nanoparticles, produced by *in situ* colloidal Knoevenagel polymerization, show advantageous properties (bright emission, colloidal/chemical stability and mesoscopic size range) that allow the successful *in vivo* application to real-time sentinel lymph node mapping in a mouse model.

Fluorescence imaging is an emerging modality of biomedical imaging with attractive features such as high sensitivity, low cost, and multiple parameters (intensity, wavelength and lifetime), as well as possibilities of multiplexing and molecular activation of signals to assess biological activities for molecular imaging.[1] Despite these unique advantages, fluorescence methods remain mainly used for small-animal studies and not generally translated into the clinic because of the photon-limiting interferences (scattering, absorption and autofluorescence) occurring in biological media. These limitations are expected to be overcome to a great extent if a breakthrough in the signal intensity is achieved by utilizing exogenous near-infrared (NIR) fluorescent probes that are orders of magnitude brighter than organic dyes currently being used. An appraisal of probe brightness is given by the number of photons detected from an individual probe that is proportional to the product of the extinction coefficient and the fluorescence quantum yield. Under absorption-limited *in vivo* conditions, the absorbing ability is the main determining factor of fluorescence brightness.[2] In this context, π-conjugated polymers hold great potential since they possess large absorptivities due to their high chromophore density. Although their bioapplications remain at the early stages of *in vitro* and *ex vivo* studies to date,[3,4] π-conjugated polymers, particularly in a densely packed nanoparticulate formulation, hold great potential for *in vivo* use owing to their organic nature of chemical constitution and water dispersibility as well as their superior light absorbing ability. In the present work, we have developed a facile preparation method for water-dispersed conjugated polymer nanoparticles to utilize them as bright nanoprobes for biomedical imaging applications. We demonstrate the successful *in vivo* application of conjugated polymer dot nanoparticles to sentinel lymph node (SLN) mapping that is a key process in SLN biopsy (SLNB) for cancer staging and surgery.[5]

In spite of the advantageous absorption properties, however, the fluorescence quantum yield of conjugated polymers, particularly in the red or NIR region, drops significantly by solidification such as nanoparticle formation, as typically observed for most organic chromophores at high concentration or in the aggregated state.[4] An exceptional case is the cyano-substituted derivatives of poly(*p*-phenylenevinylene) (CN-PPVs) that, in the aggregated film state, exhibit efficient interchain-excitonic photoluminescence in the long-wavelength region with fairly high quantum yields.[6] We thus adopted this class of polymer structure for the emissive core of the chromophore-concentrated nanoparticles, to produce water-dispersed cyanovinylene-backboned polymer dots (cvPDs) with bright solid-state fluorescence. In principle, the simultaneous achievement of high nanoscopic chromophore density and high fluorescence efficiency can lead to a significant breakthrough in the signal output from individual nanoprobes. Recently we have proven this concept by showing that nanoparticles concentrated with dyes exhibiting aggregation-enhanced fluorescence can be used as bright nanoprobes for two-photon fluorescence microscopy.[7]

Surfactant-stabilized cvPDs were directly synthesized *via in situ* colloidal polymerization in the aqueous phase without using any harmful organic solvents. For that, hydrophobic monomers (aromatic dialdehydes and diacetonitriles) were dissolved in a neat liquid surfactant (Tween 80) and then micellized in water, to allow base-catalyzed Knoevenagel polymerization to occur in the nanoscopic nonpolar interior of the micelles (Fig. 1a). The resulting fluorescence color of the cvPDs was readily tuned throughout the broad spectral window by varying the aromatic structure of the monomers (Fig. 1a; see also Fig. S1 in ESI†). Typical of common conjugated polymers, cvPDs have large Stokes shifts with minimal spectral overlaps between the absorption and emission bands, which minimize fluorescence loss by self-absorption in the chromophore-concentrated condition. Similar to quantum dots,[2] broad absorption profiles of cvPDs allow single-wavelength excitation of multicolor fluorescence, useful for simultaneous imaging of plural molecular targets (Fig. 1b). Even under UV excitation, by which autofluorescence from a live mouse would be significant, the fluorescence spots of subcutaneously injected cvPDs were clearly distinguished from the background in terms of color and brightness, indicating their potential for multicolor *in vivo* imaging.

Near-IR (NIR) emissive cvPDs were studied for *in vivo* use. The dispersion stability is attributed to the steric stabilization by residual Tween 80 left after dialysis against water. It should

[a] *Biomedical Research Center, Korea Institute of Science and Technology, 39-1 Hawolgok-dong, Seongbuk-gu, Seoul 136-791, Korea. E-mail: sehoonkim@kist.re.kr*
[b] *Basic Medical Sciences and Biomedical Engineering, Bindley Bioscience Center and Birck Nanotechnology Center, Purdue University, West Lafayette, Indiana 47907, USA*

† Electronic supplementary information (ESI) available: Experimental details and supplementary figures showing spectral, colloidal and biomedical properties of cvPDs; QuickTime movie demonstrating real-time fluorescence tracking of intradermally injected NIR-cvPDs in a mouse. See DOI: 10.1039/b923309a

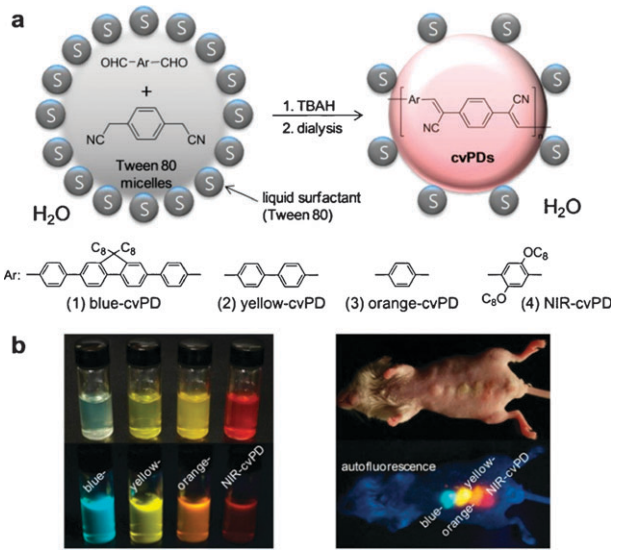

Fig. 1 (a) Schematic diagram depicting colloidal synthesis of cyanovinylene-backboned polymer dots (cvPDs) through tetrabutylammonium hydroxide (TBAH)-catalyzed Knoevenagel condensation in the hydrophobic core of solvent-free aqueous micelles. (b) True-color photographs of water-dispersed cvPDs (left) and a cvPD-injected live mouse (right) under room light (top) and UV excitation at 365 nm for fluorescence (bottom).

be noted that NIR-cvPDs are not able to be prepared by nanoprecipitation or miniemulsion methods utilizing pre-synthesized polymer solutions[4,8] because the core-constituting CN-PPV derivative is hardly soluble in organic solvents,[9] indicating the usefulness of *in situ* colloidal synthesis. The number-weighted hydrodynamic diameter of NIR-cvPDs measured by dynamic light scattering (DLS) has a size distribution of 60.3 ± 14.2 nm (see Fig. S2 in ESI†). Transmission electron microscopy (TEM) images showed high-electron-density semiconducting nanoparticles with a polydisperse size distribution of below 50 nm (Fig. 2a). NIR-cvPDs exhibit a broad absorption band and a large Stokes-shifted red-to-NIR fluorescence emission peaking at 693 nm with a quantum yield of 21% (Fig. 2b). It is noted that a significant spectral component in the visible region remains, rendering the fluorescence of the NIR-cvPDs red. The mass extinction coefficient (a light absorptivity per mass concentration representing the light gathering power per injection dose) was estimated to be as high as 21 300 $cm^2\ g^{-1}$ at the absorption maximum (465 nm). The colloidal dispersion and optical properties of NIR-cvPDs were well maintained over time in 100% serum at 37 °C. No significant changes in fluorescence intensity and scattering, owing to chemical degradation or particle aggregation, were observed during serum incubation of 8 h (see Fig. S3 in ESI†). The chemical and colloidal stability in bodily fluid suggest that the intense NIR signal of NIR-cvPDs (by virtue of high absorptivity and reasonable fluorescence efficiency) can be utilized for *in vivo* uses.

To assess the potential of NIR-cvPDs for *in vivo* imaging, we explored SLN mapping in a mouse model by fluorescence tracking. SLN is the first group of lymph nodes receiving metastatic cancer cells by direct lymphatic drainage from a primary tumor. Fast and accurate identification of SLNs is

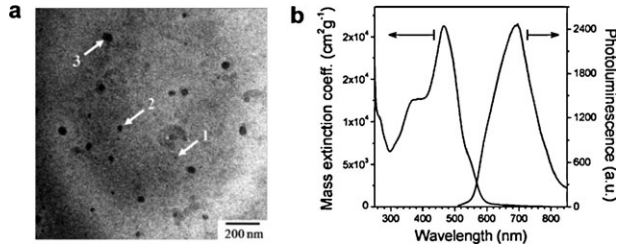

Fig. 2 (a) TEM image of NIR-cvPDs. Nanoparticles representing different size distributions are indicated: (1) 7.2 ± 0.9, (2) 25.7 ± 4.3 and (3) 47.8 ± 5.0 nm (mean ± s.d.). (b) Mass extinction coefficient and photoluminescence spectra of water-dispersed NIR-cvPDs.

thus of clinical importance for the success of cancer staging and surgery by SLNB,[5] which demands improvements over current methods based on blue dyes or radioactive colloids. The utilizations of inorganic nanomaterials are examples of studies for improved lymph node imaging.[10] NIR-cvPDs are another promising organic candidate, because their size range is optimal for lymphatic drainage and lymph node retention of colloids.[11] When NIR-cvPDs were injected intradermally into the forepaw pad of a mouse, fast movement of the fluorescence signal along lymphatic vessels could be clearly detected by a digital imaging system (Fig. 3a). Immediately after injection, NIR-cvPDs drained rapidly from the interstitial site of injection into the lymphatics and the front of the migration arrived at an axillary node in *ca.* 1 min. Subsequently migrating entities accumulated at the regional lymph node without any sign of outflow toward the next tier nodes, to give clear-cut SLN images. The whole procedure was also able to be monitored in real time using a high-speed imaging system, to offer visible guidance allowing accurate identification of the SLN position in an observational period that is short enough to be acceptable in an operating suite (see the QuickTime video in the ESI†). Importantly, the NIR-cvPD fluorescence was so intense that the dot-accumulated superficial axillary node was non-invasively discernable even by naked eye, with only 1.7 μg of the injected dose and 1–2 mW cm^{-2} of the illumination at 365 nm (Fig. 3b). After surgical dissection, the precise position and size of two SLNs (axillary and lateral thoracic nodes) as well as lymphatic vessels were more vividly recognized by fluorescence at the surgical site (Fig. 3c). Guided by intra-operative fluorescence views under a handheld UV lamp, surgical resection of the two SLNs for the histologic study could be readily completed in a minimally invasive way, as confirmed by high-sensitivity imaging inspection (see Fig. S4 and S5a in ESI†).

Biodistribution of the intradermally injected NIR-cvPDs was evaluated by *ex vivo* fluorescence imaging of resected organs, lymph nodes and the rest of the body (see Fig. S5a and S5b in ESI†). At necropsy on the seventh day after administration, strong fluorescence was observed only at the injection site (forepaw) and in the two nodes resected from the side of injection, indicating that the lymphatically drained NIR-cvPDs were efficiently trapped in the SLNs without entering the subsequent lymphatic and blood circulations. From the fluorescence intensity ratio between the footpad and the resected nodes at 60 min post-administration, the SLN uptake value was estimated to be 24% of the injected

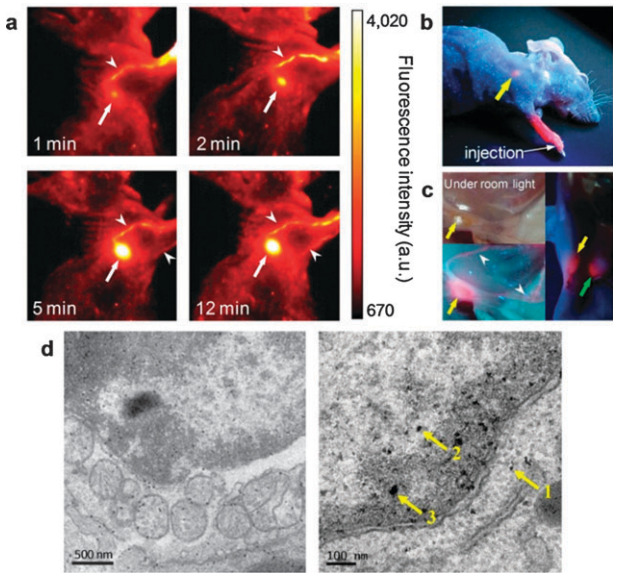

Fig. 3 (a) Pseudo-color NIR fluorescence images of a mouse (n = 10) injected intradermally with NIR-cvPDs (10 μL of 1.7 mg mL^{-1}) into the right paw. Imaging time points after injection are shown. Arrows and arrowheads indicate axillary lymph node and lymphatic vessels, respectively. The filter set used is TRITC excitation (535 nm) and Cy5.5 emission (700 nm). (b–c) True-color fluorescence photographs of a cvPD-injected mouse (10 μL of 0.17 mg mL^{-1}, intradermally into the right paw), taken under UV excitation by a 365 nm handheld lamp (1–2 mW cm^{-2}). The mouse was photographed non-invasively at 90 min post-injection (b) and subjected to incision for fluorescence-guided surgical inspection (c). Two SLNs, axillary and lateral thoracic nodes, and lymphatic vessels are indicated by yellow, green arrows and arrowheads, respectively. (d) Low (left) and high (right) magnification TEM images of cells in the dot-entrapped SLN sinus. Numbered are representative nanoparticles keeping the size distributions observed *in vitro* (Fig. 2a).

dose (see Fig. S6 in ESI†). It is noted that the evaluated high uptake efficiency might be an overestimation by the under-estimated emission intensity from the skin-covered forepaw of relatively larger volume. Histological analysis of the nodes demonstrated that the entrapped NIR-cvPDs were confined to the sinusoidal region that is the most likely location where foreign substances such as metastatic cancer cells would be found (see Fig. S5c in ESI†). The uptake by cells in the sinuses is responsible for the retention of NIR-cvPDs in the SLNs, as manifested in the electron microscopic images where the polymer dots appear to be distributed throughout the whole intracellular area in a non-aggregated form (Fig. 3d). These data suggest that fast lymphatic drainage with high SLN uptake efficiency is attributed to the steric stabilization[11] of the dots imposed by the surface-adsorbed surfactants. This colloidal stabilization minimizes the interaction with interstitial substances as well as the self-agglomeration in bodily fluid to allow the majority of the dots to retain the initial *in vitro* size range optimal for SLN mapping.

In summary, we have constructed cyanovinylene-backboned conjugated polymer dot nanoparticles (cvPDs) as *in vivo* nanoprobes. cvPDs provide attractive features: (1) high nanoscopic chromophore density and high fluorescence efficiency affords outstanding signal brightness. (2) Single-step *in situ* polymerization in solvent-free micelles under mild conditions offers ease of preparation for chemically and colloidally stable nanoprobes, as opposed to the harsh conditions and multiple processes often needed for inorganic nanomaterials. The effective SLN mapping with NIR-cvPDs provides a possibility for real-time optical guidance, by which surgeons can precisely identify superficial SLNs non-invasively or reveal deep SLNs by tracing the fluorescently visualized lymphatics during surgery. We believe that the potential of cvPDs is worthy of further optimization of performance as well as toxicity evaluation for clinical translation.

This work was supported by the Global Research Laboratory (GRL) program and the Real-Time Molecular Imaging Project funded by the Korea Ministry of Education, Science and Technology (MEST) and by the Intramural Research Program of KIST.

Notes and references

1 R. Weissleder and M. J. Pittet, *Nature*, 2008, **452**, 580; K. Park, S. Lee, E. Kang, K. Kim, K. Choi and I. C. Kwon, *Adv. Funct. Mater.*, 2009, **19**, 1553.
2 X. H. Gao, Y. Y. Cui, R. M. Levenson, L. W. K. Chung and S. M. Nie, *Nat. Biotechnol.*, 2004, **22**, 969.
3 B. Liu and G. C. Bazan, *Proc. Natl. Acad. Sci. U. S. A.*, 2005, **102**, 589; J. H. Moon, W. McDaniel, P. MacLean and L. F. Hancock, *Angew. Chem., Int. Ed.*, 2007, **46**, 8223; C. Wu, B. Bull, K. Christensen and J. McNeill, *Angew. Chem., Int. Ed.*, 2009, **48**, 2741; C. J. Sigurdson, K. P. R. Nilsson, S. Hornemann, G. Manco, M. Polymenidou, P. Schwarz, M. Leclerc, P. Hammarström, K. Wüthrich and A. Aguzzi, *Nat. Methods*, 2007, **4**, 1023.
4 C. Wu, B. Bull, C. Szymanski, K. Christensen and J. McNeill, *ACS Nano*, 2008, **2**, 2415.
5 J. W. Jakub, S. Pendas and D. S. Reintgen, *Oncologist*, 2003, **8**, 59.
6 N. C. Greenham, S. C. Moratti, D. D. C. Bradley, R. H. Friend and A. B. Holmes, *Nature*, 1993, **365**, 628; I. D. W. Samuel, G. Rumbles and C. J. Collison, *Phys. Rev. B: Condens. Matter*, 1995, **52**, R11573.
7 S. Kim, H. E. Pudavar, A. Bonoiu and P. N. Prasad, *Adv. Mater.*, 2007, **19**, 3791; S. Kim, H. Huang, H. E. Pudavar, Y. Cui and P. N. Prasad, *Chem. Mater.*, 2007, **19**, 5650; S. Kim, T. Y. Ohulchanskyy, H. E. Pudavar, R. K. Pandey and P. N. Prasad, *J. Am. Chem. Soc.*, 2007, **129**, 2669.
8 K. Landfester, R. Montenegro, U. Scherf, R. Günter, U. Asawapirom, S. Patil, D. Neher and T. Kietzke, *Adv. Mater.*, 2002, **14**, 651.
9 J. Liao and Q. Wang, *Macromolecules*, 2004, **37**, 7061.
10 S. Kim, Y. T. Lim, E. G. Soltesz, A. M. De Grand, J. Lee, A. Nakayama, J. A. Parker, T. Mihaljevic, R. G. Laurence, D. M. Dor, L. H. Cohn, M. G. Bawendi and J. V. Frangioni, *Nat. Biotechnol.*, 2004, **22**, 93; B. Ballou, L. A. Ernst, S. Andreko, T. Harper, J. A. J. Fitzpatrick, A. S. Waggoner and M. P. Bruchez, *Bioconjugate Chem.*, 2007, **18**, 389; K. H. Song, C. Kim, C. M. Cobley, Y. Xia and L. V. Wang, *Nano Lett.*, 2009, **9**, 183.
11 S. M. Moghimi and A. R. Rajabi-Siahboomi, *Prog. Biophys. Mol. Biol.*, 1996, **65**, 221.